A general phase transition model for vehicular traffic

Sebastien Blandin, Dan Work, Paola Goatin, Benedetto Piccoli, Alexandre Bayen

A GENERAL PHASE TRANSITION MODEL FOR VEHICULAR TRAFFIC

S. BLANDIN *, D. WORK †, P. GOATIN ‡, B. PICCOLI §, AND A. BAYEN ¶

Abstract. An extension of the Colombo phase transition model is proposed. The congestion phase is described by a two-dimensional zone defined around an equilibrium flux known as the classical fundamental diagram. General criteria to build such a set-valued fundamental diagram are enumerated, and instantiated on several equilibrium fluxes with different concavity properties. The solution of the Riemann problem in the presence of phase transitions is obtained through the construction of a Riemann solver, which enables the definition of the solution of the Cauchy problem using wavefront tracking. The free-flow phase is described using a Newell-Daganzo fundamental diagram, which allows for a more tractable definition of phase transition compared to the original Colombo phase transition model. The accuracy of the numerical solution obtained by a modified Godunov scheme is assessed on benchmark scenarios for the different flux functions constructed.

Key words. partial differential equations, hyperbolic systems of conservation laws, macroscopic highway traffic flow model, phase transition, numerical scheme, riemann solver

AMS subject classifications. 35L65, 35F25, 65M12, 90B20, 76T99

1. Introduction. First order scalar models of traffic. Hydrodynamic models of traffic go back to the 1950's with the seminal work of Lighthill, Whitham and Richards [31, 38], who built the first model of the evolution of vehicle density on the highway using a first order scalar hyperbolic *partial differential equation* (PDE) referred to as the LWR PDE. Their model relies on the knowledge of an empirically measured *flux function*, also called the *fundamental diagram* in transportation engineering, for which measurements go back to 1935 with the pioneering work of Greenshields [23]. Numerous other flux functions have since been proposed in the hope of capturing effects of congestion more accurately, in particular: Greenberg [22], Underwood [43], Newell-Daganzo [12, 34], and Papageorgiou [46]. The existence and uniqueness of an *entropy* solution to the *Cauchy problem* [39] for the class of scalar conservation laws to which the LWR PDE belong go back to the work of Oleinik [35] and Kruzhkov [27], (see also the seminal article of Glimm [20]), which was extended later to the *initial-boundary value problem* [2], and specifically instantiated for the scalar case with a concave flux function in [29], in particular for traffic in [40]. Numerical solutions of the LWR PDE go back to the seminal *Godunov scheme* [21, 30], which was shown to converge to the entropy solution of the first order hyperbolic PDE (in particular the LWR PDE). In the transportation engineering community, the *Godunov scheme* is known under the name of *Cell Transmission Model* (CTM), which was brought to this field by Daganzo in 1995 [12, 13], and is one of the most used discrete traffic flow models in the literature today [6, 15, 24, 32, 33, 36, 45].

*Ph.D. student, Systems Engineering, Department of Civil and Environmental Engineering, University of California, Berkeley, USA. Email: blandin@berkeley.edu. Corresponding author.

†Ph.D. student, Systems Engineering, Department of Civil and Environmental Engineering, University of California, Berkeley, USA. Email: dbwork@berkeley.edu.

‡Assistant Professor, Institut de mathématiques de Toulon et du Var, I.S.I.T.V., Université du Sud Toulon - Var, La Valette du Var, France. E-mail: goatin@univ-tln.fr

§Research Director, Istituto per le Applicazioni del Calcolo 'M. Picone', Roma, Italy. Email: bpiccoli@iac.cnr.it

¶Assistant Professor, Systems Engineering, Department of Civil and Environmental Engineering, University of California, Berkeley, USA. Email:bayen@berkeley.edu

Set-valued fundamental diagrams. The assumption of a Greenshields fundamental diagram or a triangular *fundamental diagram*, which significantly simplifies the analysis of the model algebraically, led to the aforementioned theoretical developments. Yet, experimental data clearly indicates that while the free flow part of a fundamental diagram can be approximated fairly accurately by a straight line, the congested regime is set valued, and can hardly be characterized by a single curve [44]. An approach to model the set-valuedness of the congested part of the fundamental diagram consists in using a second equation coupled with the mass conservation equation (i.e. the LWR PDE model). Such models go back to Payne [37] and Whitham [47] and generated significant research efforts, but led to models with inherent weaknesses pointed out by del Castillo [17] and Daganzo [14]. These weaknesses were ultimately addressed in several responses [1, 36, 48], leading to sustained research in this field.

Motivation for a new model. Despite the existing research, modeling issues remain in most 2×2 models of traffic available today. For instance, the *Aw-Rascle* model [1] raises issues about the validity of the physics of the highway [19], such as the existence of a zero velocity achieved below jam density. In agreement with the remarks from Kerner [25, 26] affirming that traffic flow presents three different behaviors, *free-flow*, *wide moving jams*, and *synchronized flow*, Colombo proposed a 2×2 phase transition model [9, 10] which considers *congestion* and *free-flow* in traffic as two different phases, governed by distinct evolutionary laws. The well-posedness of this model was proved in [11] using *wavefront tracking* introduced by Bressan [4]. In the phase transition model, the evolution of the parameters is governed by two distinct dynamics; in *free-flow*, the Colombo phase transition model is a classical first order model (LWR PDE), whereas in *congestion* a similar equation governs the evolution of an additional state variable, the *linearized momentum* q. The motivation for an extension of the 2×2 phase transition model comes from the following:

(i) *Phases gap.* The phase transition model introduced by Colombo in [9] uses a Greenshields flux function to describe *congestion*, which despite its simple analytical expression yields a fundamental diagram which is not connected and thus a complex definition of the solution of the Riemann problem between two different phases. We solve this problem by introducing a Newell-Daganzo flux function for *free-flow*, which creates a non-empty intersection between the congested phase and the *free-flow* phase, called *metastable phase*. It alleviates the inconvenience of having to use a shock-like phase transition in many cases of the Riemann problem with two different phases.

(ii) *Definition of a general class of set-valued fundamental diagrams.* The work achieved in [9] enables the definition of a set-valued fundamental diagram for the expression of the velocity function introduced. However, experimental data shows that the fundamental diagram depends on space and time, and the congested domain changes accordingly. In this article we provide a general method to build an arbitrary set-valued fundamental diagram which in a special case corresponds to the fundamental diagram introduced in [9]. This enables one to define a custom-made set-valued fundamental diagram.

Organization of the article. The rest of the article is organized as follows. Section 2 presents the fundamental features of the Colombo phase transition model [10], which serves as the basis for the present work. In § 3, we introduce the modifications to the Colombo phase transition model, and introduce the notion of *equilibrium* which provides the basis for the construction of a class of 2×2 traffic models. We also assess general conditions which enable us to extend the results obtained for the original Colombo phase transition model to these new models. Finally, this section

presents a modified *Godunov scheme* which can be used to solve the equations numerically. The two following sections instantiate the constructed class of models for two specific flux functions, which are the Newell-Daganzo (affine) flux function (§ 4) and the Greenshields (parabolic concave) flux function (§ 5). Each of these sections includes the discussion of the choice of parameters needed for each of the models, the solution of the Riemann problem, and a validation of the numerical results using a benchmark test for which wavefront tracking methods enable an almost exact solution used for comparison with the numerical solution. Finally, § 6 presents some concluding remarks.

2. The Colombo phase transition model. The original Colombo phase transition model [9, 10] is a set of two coupled PDEs respectively valid in a *free-flow* regime and *congested* regime:

$$\begin{cases} \partial_t \rho + \partial_x(\rho\, v_f(\rho)) = 0 & \text{in free-flow } (\Omega_f) \\ \begin{cases} \partial_t \rho + \partial_x(\rho\, v_c(\rho,q)) = 0 \\ \partial_t q + \partial_x((q-q^*)\, v_c(\rho,q)) = 0 \end{cases} & \text{in congestion } (\Omega_c) \end{cases} \tag{2.1}$$

where the states variable ρ and q note respectively the density and the *linearized momentum* [10]. Ω_f and Ω_c are the respective domains of validity of the free-flow and congested equations of the model and are explicited below. The term q^* is a parameter characteristic of the road under consideration. An empirical model must be used to express the velocity v as a function of density in free-flow: $v := v_f(\rho)$, and as a function of density and linearized momentum in congestion: $v := v_c(\rho, q)$. Following usual choices for traffic applications [18], the functions below are used:

$$v_f(\rho) = \left(1 - \frac{\rho}{R}\right) V \quad \text{and} \quad v_c(\rho, q) = \left(1 - \frac{\rho}{R}\right) \frac{q}{\rho}$$

where R is the maximal density or *jam density* and V is the maximal *free-flow speed*. The relation for free-flow is the *Greenshields* model [23] mentioned earlier while the second relation has been introduced in [9]. As Ω_c should be an invariant domain [39] for the congested dynamics from system (2.1), and according to the definition of v, the free-flow and congested domains are defined as follows:

$$\begin{cases} \Omega_f = \{(\rho, q) \in [0, R] \times [0, +\infty[\ \ , v_f(\rho) \geq V_{f-}\ \ ,\ \ q = \rho\, V\} \\ \Omega_c = \left\{(\rho, q) \in [0, R] \times [0, +\infty[\ \ , v_c(\rho, q) \leq V_{c+}\ \ ,\ \ \frac{Q^- - q^*}{R} \leq \frac{q - q^*}{\rho} \leq \frac{Q^+ - q^*}{R}\right\} \end{cases}$$

where V_{f-} is the minimal velocity in free-flow and V_{c+} is the maximal velocity in congestion such that $V_{c+} < V_{f-} < V$. R is the maximal density and Q^- and Q^+ are respectively the minimal and maximal value for q. The fundamental diagram in (ρ, q) coordinates and in $(\rho, \rho\, v)$ coordinates is presented in figure 2.1.

REMARK 2.1. For the system to be strictly hyperbolic, one must have $\lambda_1(\rho, q) \neq \lambda_2(\rho, q)$ for all $(\rho, q) \in \Omega_c$.

REMARK 2.2. The 1-Lax curves are straight lines going through $(0, q^*)$ in (ρ, q) coordinates which means along these curves shocks and rarefaction exist and coincide [41]. One must note that the 1-Lax field is not *genuinely non-linear* (GNL). Indeed the 1-Lax curves are *linearly degenerate* (LD) for $q = q^*$ and GNL otherwise with rarefaction waves propagating in different directions relatively to the eigenvector depending on the sign of $q - q^*$. The 2-Lax curves which are straight lines going through the origin in $(\rho, \rho\, v)$ coordinates, are always LD.

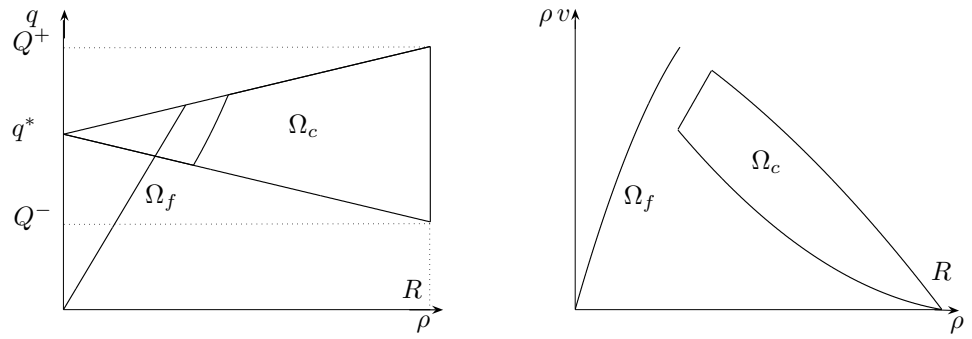

FIG. 2.1. ***Colombo phase transition model. Left**: Fundamental diagram in state space coordinates (ρ, q). **Right**: Fundamental diagram in density flux coordinates $(\rho, \rho\, v)$.*

3. Extension of the Colombo phase transition model. The approach developed by Colombo provides a fundamental diagram which is thick in congestion (figure 2.1), and thus can model clouds of points observed experimentally (figure 3.1). We propose to extend the Colombo approach by considering the second equation in

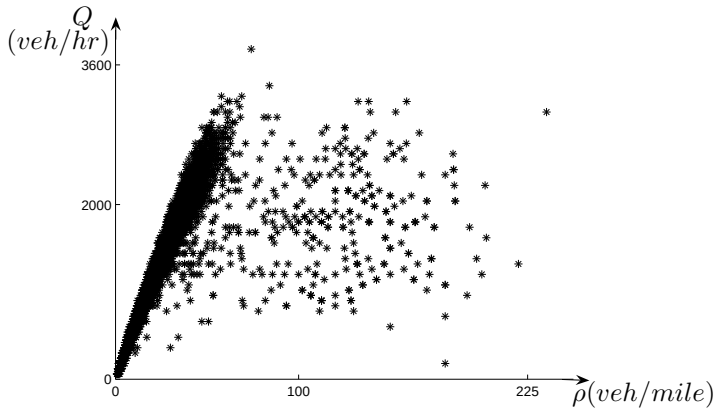

FIG. 3.1. ***Fundamental diagram in density flux coordinates from a street in Rome.** In congestion (high densities) the flux is multi-valued. Count C and velocity v were recorded every minute during one week. Flux Q was computed from the count. Density ρ was computed from flux and velocity according to the expression $Q = \rho\, v$ (see [3] for an extensive analysis of this dataset).*

congestion as modeling a perturbation [48, 49]. The *equilibrium* (Definition 3.1) would be the usual one-dimensional fundamental diagram, with dynamics described by the conservation of mass. Perturbations can move the system off equilibrium, leading the diagram to span a two-dimensional area in congestion. A single-valued map is able to describe the free-flow mode, which is therefore categorized as an equilibrium.

DEFINITION 3.1. *We call equilibrium the set of states for which the perturbation vanishes. In the following we respectively refer to the equilibrium velocity and equilibrium flux as the velocity and flux at equilibrium.*

In this article we present analytical requirements on the velocity function in congestion which, given the work done in [10], enable us to construct a 2×2 phase transition model. These models provide support for a physically correct, mathematically well-

posed initial-boundary-value problem which can model a two parameter dependent congestion on a stretch of highway. To be accurate, the two dimensional zone must be related to the reality of the local traffic nature, which is not always possible with the original Colombo phase transition model. Given the requirements described in § 3.1 and § 3.2.2, one is able to build a custom-made phase transition model. Note that unlike the Colombo phase transition model, the free-flow and congested domain of the fundamental diagram proposed in the present work are connected, as illustrated in figure 3.2. This feature enables one to define solutions in a simpler way and leads to a more straightforward numerical resolution. Moreover, the models derived need less parameters and thus are easier to calibrate. Finally, it is consistent with the fact that a gap between phases is not observed in experimental data, see figure 3.1.

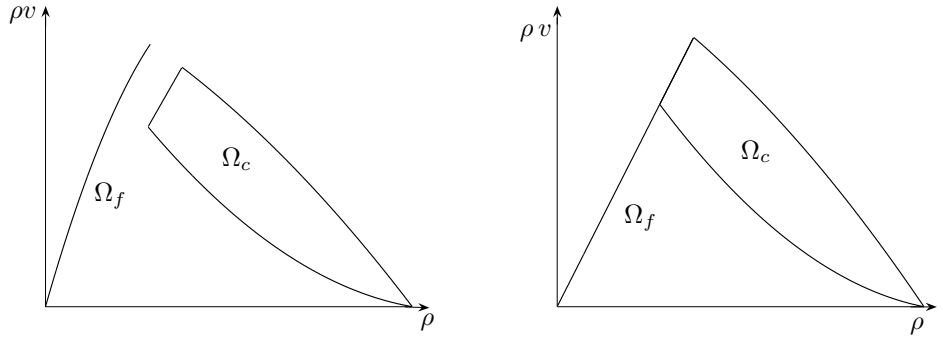

FIG. 3.2. ***Different free-flow phases. Left:*** *Fundamental diagram from the original Colombo phase transition model.* ***Right:*** *Fundamental diagram of the model derived in the present article in the particular case of a Newell-Daganzo flux-density relation for congestion at equilibrium.*

3.1. Analysis of the equilibrium. We consider the density variable ρ to belong to the interval $[0, R]$ where R is the maximal density. Given the *critical density* [1] σ in $(0, R]$, we define the equilibrium velocity $v^{eq}(\cdot)$ on $[0, R]$ by:

$$v^{eq}(\rho) := \begin{cases} V & \text{for } \rho \in [0, \sigma] \\ v_c^{eq}(\rho) & \text{for } \rho \in [\sigma, R] \end{cases}$$

where V is the free-flow speed and $v_c^{eq}(\cdot)$ is in $C^\infty((\sigma, R), \mathbf{R}^+)$. It is important to note that $v_c^{eq}(\cdot)$ is a function of ρ only, as it is the case for the classical fundamental diagram. The equilibrium flux $Q^{eq}(\cdot)$ is thus defined on $[0, R]$ by:

$$Q^{eq}(\rho) := \rho\, v^{eq}(\rho) = \begin{cases} Q_f(\rho) := \rho\, V & \text{for } \rho \in [0, \sigma] \\ Q_c^{eq}(\rho) := \rho\, v_c^{eq}(\rho) & \text{for } \rho \in [\sigma, R]. \end{cases}$$

In agreement with traffic flow features, the congested equilibrium flux $Q_c^{eq}(\rho)$ must satisfy the following requirements (which are consistent with the ones given in [16]).

(i) *Flux vanishes at the maximal density*: $Q_c^{eq}(R) = 0$.

This condition encodes the physical situation in which the jam density has been reached. The corresponding velocity and flux of vehicles on the highway is zero.

[1] Density for which the flux is maximal in scalar models. At this density the system switches between free-flow and congestion.

(ii) *Flux is a decreasing function of density in congestion*: $dQ_c^{eq}(\rho)/d\rho \leq 0$.
This is required as a defining property of congestion. It implies that $dv_c^{eq}(\rho)/d\rho \leq 0$.

(iii) *Continuity of the flux at the critical density*: $Q_c^{eq}(\sigma) = Q_f(\sigma)$.
Even if some models account for a discontinuous flux at capacity, the *capacity drop* phenomenon [26], we assume as most of the transportation community that the flux at equilibrium is a continuous function of density.

(iv) *Concavity of the flux in congestion*: $Q_c^{eq}(\cdot)$.
The flux function at equilibrium $Q_c^{eq}(\cdot)$ must be concave on $[\sigma, \sigma_i]$ and convex on $[\sigma_i, R]$ where σ_i is in $(\sigma, R]$. Given the plots experimentally obtained for congestion (figure 3.1), it is not clear in practice if the equilibrium flux is concave or convex in congestion. The assumption made here is detailed in remark 3.2.

REMARK 3.2. A physical interpretation can be given to the concavity of the flux function. In congestion, when the density increases toward the maximal density, the velocity decreases toward zero. This yields the decreasing slope of the flux in congestion. The way in which drivers velocity decreases impacts the concavity of the flux, as per the expression of the second derivative of the equilibrium flux function, $d^2Q_c^{eq}(\rho)/d\rho^2 = \rho\, d^2v_c^{eq}(\rho)/d\rho^2 + 2\, dv_c^{eq}(\rho)/d\rho$.

(i) If for a given density increase, the drivers reduce their speed more at high densities than at low densities (modeling aggressive drivers who wait until high density to reduce speed), then the velocity function is concave and the flux function is concave.

(ii) If the drivers reduce their speeds less at high densities than at low densities (modeling careful drivers who have reduced speed at low densities), then the velocity function is convex, and if its convexity is great enough, the flux function is convex.

(iii) An affine flux is given by a hyperbolic velocity function.
The assumption above that if the flux is convex for a low congested density then it can not be concave for a higher congested density means that we assume that drivers tend to be more careful when congestion increases.

REMARK 3.3. In this article we instantiate the general model proposed on the most common equilibrium flux functions, i.e. linear or concave, but the framework developed here applies to flux functions with changing concavity such as the Li flux function [28] and yields a significantly more complex analysis.

EXAMPLE 3.4. Assuming the system is always at equilibrium, we have:

$$\partial_t \rho + \partial_x Q(\rho) = 0 \tag{3.1}$$

for $\rho \in [0, R]$ and with $Q(\cdot) \equiv Q_f(\cdot)$ in free-flow and $Q(\cdot) \equiv Q_c^{eq}(\cdot)$ in congestion. Equation (3.1) is the classical LWR equation. In traffic theory, a triangular flux function $Q(\cdot)$ is called *Newell-Daganzo* flux [12, 34] and yields the fundamental diagram drawn in figure 3.3 (left), whereas a parabolic flux function is called a *Greenshields* flux [23] and yields the fundamental diagram shown in figure 3.3 (right).

3.2. Analysis of the perturbation.

3.2.1. Model outline. In this section we introduce a perturbation to the equilibrium velocity in congestion as follows:

$$v_c(\rho, q) = v_c^{eq}(\rho)\,(1 + q) \tag{3.2}$$

where $\rho \in [0, R]$, and $q \in [q_-, q_+]$ is the perturbation, which can be positive or negative. The equilibrium corresponds to $q = 0$, and the evolution of (ρ, q) is described

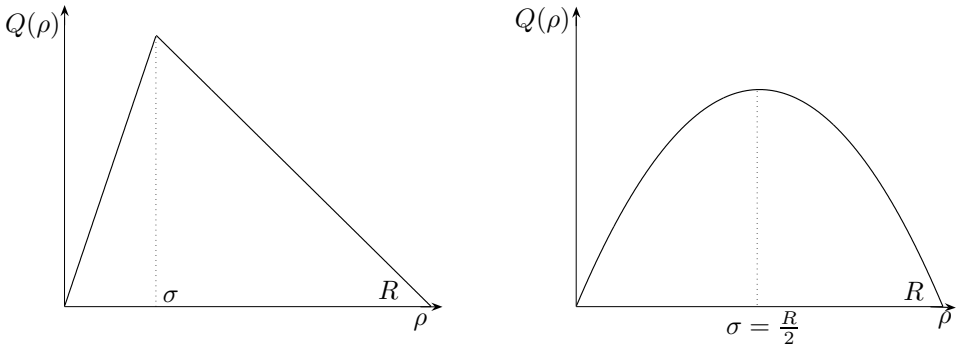

FIG. 3.3. ***Fundamental diagram at equilibrium in density flux coordinates. Left****: Newell-Daganzo flux.* ***Right****: Greenshields flux.*

similarly to the classical Colombo phase transition model [10] by:

$$\begin{cases} \partial_t \rho + \partial_x(\rho\, v) = 0 & \text{in free-flow} \\ \begin{cases} \partial_t \rho + \partial_x(\rho\, v) = 0 \\ \partial_t q + \partial_x(q\, v) = 0 \end{cases} & \text{in congestion} \end{cases} \tag{3.3}$$

with the following expression of the velocity:

$$v = \begin{cases} v_f(\rho) := V & \text{in free-flow} \\ v_c(\rho, q) & \text{in congestion.} \end{cases} \tag{3.4}$$

The perturbed velocity function defines the velocity in congestion whereas a Newell-Daganzo function describes the velocity in free-flow. The system (3.3)- (3.4) differs from the one used by Colombo on three points:

(i) We set the equilibrium to be at $q^* = 0$.
(ii) We use a Newell-Daganzo flux function in free-flow.
(iii) We do not further specify the expression of the function v_c at this point.

DEFINITION 3.5. *The flux in congestion on Ω_c is $Q_c(\rho, q) = \rho\, v_c(\rho, q)$.*

The analytical expression of the free-flow and congested domains as explicited in (3.5) is motivated by the analysis conducted in table 3.1 and the necessity for these domains to be invariants [39] for the dynamics (3.3) in order to have a well-defined Riemann solver [42].

$$\begin{cases} \Omega_f = \{(\rho, q) \mid (\rho, q) \in [0, R] \times [0, +\infty[\ \ , v_c(\rho, q) = V\ \ ,\ \ 0 \leq \rho \leq \sigma_+\} \\ \Omega_c = \left\{(\rho, q) \mid (\rho, q) \in [0, R] \times [0, +\infty[\ \ , v_c(\rho, q) < V\ \ ,\ \ \frac{q^-}{R} \leq \frac{q}{\rho} \leq \frac{q^+}{R}\right\} \end{cases} \tag{3.5}$$

σ_+ is defined by $v_c(\sigma_+, \sigma_+\, q_+/R) = V$. A definition of the whole set of parameters can be found in § 3.4 (See also illustration in figure 3.4 for the Newell-Daganzo case.).

DEFINITION 3.6. *We define the set $\{(\rho, q) \mid v_c(\rho, q) = V\ \ ,\ \ \sigma_- \leq \rho \leq \sigma_+\}$ as the set of metastable states. We choose to place it in the free-flow domain for convenience in the definition of the Riemann solver. However, the states it contains can be considered to belong to the congestion domain.*

EXAMPLE 3.7. For a Newell-Daganzo flux for both congestion equilibrium and free-flow, the fundamental diagram obtained has the shape presented in figure 3.4.

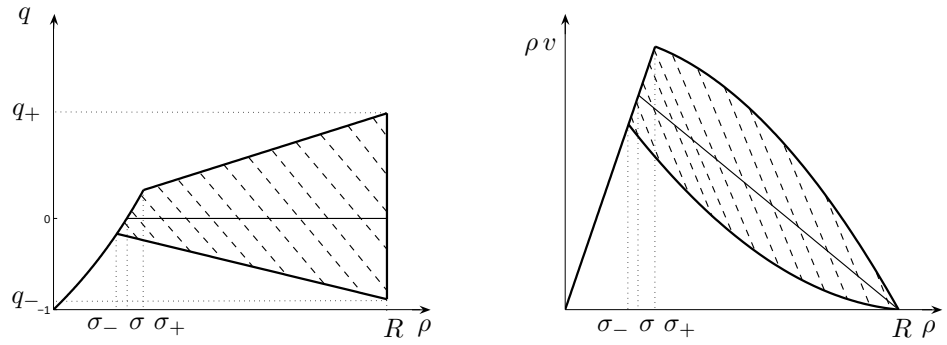

FIG. 3.4. ***Newell-Daganzo equilibrium flux function. Left:*** *Fundamental diagram in state space coordinates.* ***Right:*** *Fundamental diagram in flux-density coordinates. The equilibrium is the usual triangular diagram as in figure* 3.3*. A two-dimensional off-equilibrium set of parameters (striped domain) is modeled in congestion.*

REMARK 3.8. The left boundary of the congested domain is a convex curve in (ρ, q) coordinates (in figure 2.1 for the Colombo phase transition model as in figure 3.4 for the new model derived). Thus Ω_c is not convex in (ρ, q) coordinates.

The analysis of the congestion phase of the model (3.3) is outlined in table 3.1.

Eigenvalues	$\lambda_1(\rho,q) = v_c^{eq}(\rho)\,(1+q) + q\,v_c^{eq}(\rho) + \rho\,(1+q)\partial_\rho v_c^{eq}(\rho)$	$\lambda_2(\rho,q) = v_c^{eq}(\rho)\,(1+q)$
Eigenvectors	$r_1 = \begin{pmatrix} \rho \\ q \end{pmatrix}$	$r_2 = \begin{pmatrix} v_c^{eq}(\rho) \\ -(1+q)\,\partial_\rho v_c^{eq}(\rho) \end{pmatrix}$
Nature of the Lax-curves	$\nabla\lambda_1.r_1 = \rho^2\,(1+q)\partial^2_{\rho\rho} v_c^{eq}(\rho) + 2\,\rho\,(1+2\,q)\,\partial_\rho v_c^{eq}(\rho) + 2\,q\,v_c^{eq}(\rho)$	$\nabla\lambda_2.r_2 = 0$
Riemann-invariants	q/ρ	$v_c^{eq}(\rho)\,(1+q)$

TABLE 3.1

Algebraic features of the extended Colombo phase transition model for the congestion phase.

3.2.2. Physical and mathematical considerations. Physical interpretation and mathematical conditions translate into the following conditions:

CONDITION 3.9. ***Positivity of speed*** *In order to maintain positivity of $v_c(\cdot,\cdot)$ on the congested domain, one must have:*

$$\forall\, q \in [q_-, q_+] \quad 1 + q > 0 \tag{3.6}$$

which is satisfied if and only if $q_- > -1$.

CONDITION 3.10. ***Strict hyperbolicity of the congested system*** *In order for the congested part of* (3.3) *to be strictly hyperbolic, one must have:*

$$\forall\,(\rho,q) \in \Omega_c \quad \lambda_1(\rho,q), \lambda_2(\rho,q) \in \mathbf{R} \;\; \textit{and} \;\; \lambda_1(\rho,q) \neq \lambda_2(\rho,q).$$

Given the expression of the eigenvalues outlined in table 3.1*, and modulo a rearrangement, this yields:*

$$\forall\,(\rho,q) \in \Omega_c \quad \rho\,\partial_\rho v_c^{eq}(\rho) + q\,(v_c^{eq}(\rho) + \rho\,\partial_\rho v_c^{eq}(\rho)) \neq 0. \tag{3.7}$$

Since $v_c^{eq}(\cdot)$ is positive and $\rho\, v_c^{eq}(\cdot)$ is a decreasing function of ρ, this can always be satisfied for small enough values of q, and when instantiated for specific expressions of $v_c^{eq}(\cdot)$, will result in a bound on the perturbation q.

CONDITION 3.11. ***Shape of Lax curves*** *For modeling consistency, we require the 1-Lax curves to be LD or to have no more than one inflexion point (σ_i, q_i). In the latter case they should be concave for $\rho \leq \sigma_i$ and convex for $\rho \geq \sigma_i$. Since the value of $\nabla\lambda_1.r_1(\rho,q)$ is the value at (ρ,q) of the concavity of the 1-Lax-curve going through (ρ,q), the latter is given for any (ρ,q) in the congested domain, by the sign of the expression:*

$$\nabla\lambda_1.r_1 = \rho\,(2\,\partial_\rho v_c^{eq}(\rho) + \rho\,\partial^2_{\rho\rho} v_c^{eq}(\rho)) + q\,(2\,v_c^{eq} + 4\,\rho\,\partial_\rho v_c^{eq}(\rho) + \rho^2\,\partial^2_{\rho\rho} v_c^{eq}(\rho)) \quad (3.8)$$

which has the sign of the first term for q small enough. So if $2\,\partial_\rho v_c^{eq}(\rho) + \rho\,\partial^2_{\rho\rho} v_c^{eq}(\rho) > 0$ the rarefaction waves go right in the (ρ,q) or $(\rho,\rho\,v)$ plane. When $v_c^{eq}(\cdot)$ is such that $2\,\partial_\rho v_c^{eq}(\rho) + \rho\,\partial^2_{\rho\rho} v_c^{eq}(\rho) = 0$ the heading of rarefaction waves changes with the sign of q (it is the case for the classical Colombo phase transition model [10]*), and in this case the 1-curves are LD for $q = 0$.*
This condition consists in ensuring that expression (3.8) *is either identically zero (LD curve), or has no more than one zero and is an increasing function of the density.*

REMARK 3.12. One may note that condition 3.10 on the strict hyperbolicity of the system is satisfied whenever condition 3.9 on the positivity of speed is satisfied. Indeed equation (3.7) can be re-written as $\forall(\rho,q) \in \Omega_c \quad \rho\,\partial_\rho v_c^{eq}(\rho) + q\partial_\rho Q_c^{eq}(\rho) \neq 0$, which given the first term is negative, is equivalent to $\forall(\rho,q) \in \Omega_c \quad \rho\,\partial_\rho v_c^{eq}(\rho) + q\partial_\rho Q_c^{eq}(\rho) < 0$. For non-zero values of $\partial_\rho Q_c^{eq}(\rho)$, it yields $q > -\rho\,\partial_\rho v_c^{eq}(\rho)/\partial_\rho Q_c^{eq}(\rho) = -1 + v_c^{eq}(\rho)/\partial_\rho Q_c^{eq}(\rho)$ which is always satisfied when $q_- > -1$, because the second term of the right hand side is negative.

REMARK 3.13. In this model, traffic is anisotropic in the sense that no wave travels faster than vehicles ($\lambda_1(\rho,q) < \lambda_2(\rho,q) = v_c(\rho,q)$). The speed of vehicles is always positive and they stop only at maximal density.

3.3. Cauchy problem. In this section we define a solution of the Cauchy problem for the system (3.3). Following [10], we use a definition derived from [4].

DEFINITION 3.14. *Given T in $\mathbf{R}_+$, and an initial condition u_0 in $BV(\mathbf{R})$, an admissible solution of problem* (3.3) *is a function $u(\cdot,\cdot)$ in $BV([0,T)\times\mathbf{R})$ such that the following holds.*

(i) *For all t in $[0,T)$, $t \mapsto u(t,.)$ is continuous with respect to the L^1 norm.*

(ii) *For all functions φ in $C_c^1([0,T)\times\mathbf{R} \mapsto \mathbf{R})$ with compact support contained in $u^{-1}(\Omega_f)$:*

$$\int_0^T \int_{\mathbf{R}} (u(t,x)\,\partial_t\varphi(t,x) + Q_f(u(t,x))\partial_x\varphi(t,x))\,dxdt + \int_{\mathbf{R}} u_0(x)\,\varphi(0,x)dx = 0.$$

(iii) *For all functions φ in $C_c^1([0,T)\times\mathbf{R} \mapsto \mathbf{R}^2)$ with compact support contained in $u^{-1}(\Omega_c)$:*

$$\int_0^T \int_{\mathbf{R}} (u(t,x)\,\partial_t\varphi(t,x) + Q_c(u(t,x))\partial_x\varphi(t,x))\,dxdt + \int_{\mathbf{R}} u_0(x)\,\varphi(0,x)dx = 0.$$

(iv) *The set of points (t,x) for which there is a change of phase is the union of a finite number of Lipschitz curves $p_i : [0,T) \mapsto \mathbf{R}$ such that if $\exists i \neq j$ and $\exists\tau \in [0,T]$ such that $p_i(\tau) = p_j(\tau)$ then $\forall t \in [\tau,T]$ we have $p_i(t) = p_j(t)$.*

(v) *For all points* (t, x) *where there is a change of phase, let* $\Lambda = \dot{p_i}(t^+)$*, and introducing the left and right flow at* (t, x)*:*

$$F^l = \begin{cases} \rho(t, x^-)\, v_f(\rho(t, x^-)) & \text{if } \rho(t, x^-) \in \Omega_f \\ \rho(t, x^-)\, v_c(\rho(t, x^-), q(t, x^-)) & \text{if } \rho(t, x^-) \in \Omega_c \end{cases}$$

$$F^r = \begin{cases} \rho(t, x^+)\, v_f(\rho(t, x^+)) & \text{if } \rho(t, x^+) \in \Omega_f \\ \rho(t, x^+)\, v_c(\rho(t, x^+), q(t, x^+)) & \text{if } \rho(t, x^+) \in \Omega_c \end{cases}$$

the following relation must be satisfied:

$$\Lambda \cdot (\rho(t, x_+) - \rho(t, x_-)) = F_r - F_l. \tag{3.9}$$

REMARK 3.15. This definition of solution matches the standard Lax solution for an initial condition with values in Ω_f or Ω_c. Equation (3.9) is a Rankine-Hugoniot relation needed to ensure mass conservation at the phase transition. A Lax-entropy condition is added at the phase transition to ensure uniqueness. This will be used for the definition of the Riemann solver in the following sections.

THEOREM 3.16. *For all* u_0 *in BV with values in* $\Omega_f \bigcup \Omega_c$*, the problem* (3.3) *admits a solution* $u : [0, +\infty) \times \mathbf{R} \mapsto \Omega_f \bigcup \Omega_c$ *such that* $u(0, x) = u_0(x)$. The interested reader is referred to [10, 11] for a proof.

REMARK 3.17. For the initial-boundary value problem, the same result holds with an appropriate formulation of the boundary conditions [2, 29, 40].

3.4. Definition of parameters. Several parameters are used in the proposed model, which we summarize below:

(i) The free-flow speed V.
(ii) The maximal density R.
(iii) The critical density at equilibrium σ.
(iv) The critical density for the lower bound of the diagram σ_-.
(v) The critical density for the upper bound of the diagram σ_+.

These parameters can be identified from experimental data, and enable the definition of the parameters q_- and $q+$. Figure 3.4 graphically summarizes the definition of the parameters chosen. However one must note that the constraints on q_-, q_+ detailed in (3.6)-(3.7)-(3.8) translate into constraints on σ_-, σ_+, which can not be freely chosen.

3.5. Numerics.

3.5.1. Modified Godunov scheme. Because of the non-convexity of the domain $\Omega_f \cup \Omega_c$ (illustrated in figure 3.4), using the classical Godunov scheme [30] is not feasible due to the projection step of the scheme. As detailed in [7], we use a modified version of the scheme which mimics the two steps of the classical Godunov scheme and adds a final sampling step.

(i) The Riemann problems are solved on a regular time space mesh. When two space-consecutive cells do not belong to the same phase, the position of the phase transition at the next time step is computed.

(ii) The solutions are averaged on the domains defined by the position of the phase transitions issued from Riemann problems from neighboring cells (figure 3.5 and 3.6).

(iii) A sampling method is used to determine the value of the solution in each cell of the regular mesh.
This process answers the issues of the classical Godunov scheme with non-convex domains. Numerical results have shown that it gives accurate results on benchmark tests (we refer to [7] for more details on the test cases used).

3.5.2. Detail of the numerical scheme. In order to discretize time and space, we introduce a time step Δt and a space step Δx, both assumed to be constant. Let $N, M \in \mathbf{N}$, we call $x_j = j\,\Delta x$ for $j \in \mathbf{Z}$ and $t^n = n\,\Delta t$ for $n \in \mathbf{N}$. We call $x_{j-1/2} = x_j - \Delta x/2$ and we define a cell $C_j^n = \{t_n\} \times [x_{j-1/2}, x_{j+1/2}[$ which has a length Δx. We call u_j^n the value of $u := (\rho, q)$ at (t_n, x_j), and, by extension, in C_j^n.

At each time step, the speed $\nu_{j+1/2}^n$ of the phase transition between each pair of cells (C_j^n, C_{j+1}^n) is computed, by computing the solution of the Riemann problem between these two cells ($\nu_{j+1/2}^n$ equals zero if u_j^n and u_{j+1}^n belongs to the same phase). If we call $\overline{x}_{j-1/2}^{n+1} = x_{j-1/2} + \nu_{j-1/2}^n\,\Delta t$ we can define cell $\overline{C}_j^{n+1}$ as $\overline{C}_j^{n+1} = \left\{t^{n+1}\right\} \times [\overline{x}_{j-1/2}^{n+1}, \overline{x}_{j+1/2}^{n+1}[$ which has a length $\Delta\overline{x}_j^n = \overline{x}_{j+1/2}^{n+1} - \bar{x}_{j-1/2}^{n+1}$, as shown in figure 3.5 and 3.5. The solution to the Riemann problem between cells C_j^n is averaged on cells

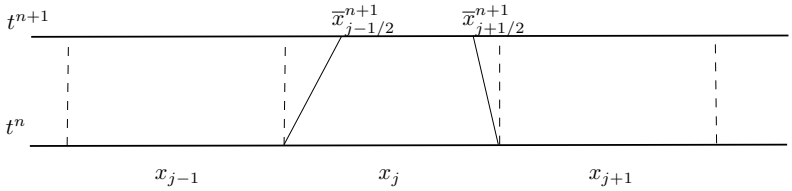

FIG. 3.5. *Phase transitions enter cell C_j^n from both sides.*

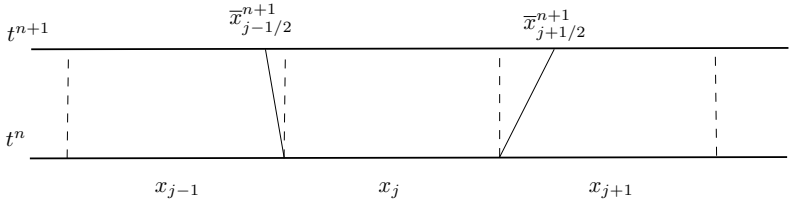

FIG. 3.6. *Phase transitions exit cell C_j^n from both sides.*

$\overline{C}_j^{n+1}$, which by construction enclose states which are either free-flowing or congested, according to the modified Godunov scheme. We define:

(i) $g\left(\nu_{j+1/2}^{n,-}, u_j^n, u_{j+1}^n\right)$ as the numerical flux between cells C_j^n and C_{j+1}^n, at $\frac{x-x_{j+1/2}}{t-t^n} = \nu_{j+1/2}^n$, and calculated at the left of the discontinuity.

(ii) $u_R(\nu_{j-1/2}^{n,+}, u_{j-1}^n, u_j^n)$ as the solution of the Riemann problem between u_{j-1}^n and u_j^n, at $\frac{x-x_{j-1/2}}{t-t^n} = \nu_{j-1/2}^n$, and calculated at the right of the discontinuity.
The averaging step of the modified Godunov scheme reads:

$$\Delta\overline{x}_j^n\,\overline{u}_j^{n+1} = \Delta x\,u_j^n - \Delta t\,\left(g\left(\nu_{j+1/2}^{n,-}, u_j^n, u_{j+1}^n\right) - \nu_{j+1/2}^n\,u_R\left(\nu_{j+1/2}^{n,-}, u_j^n, u_{j+1}^n\right)\right)$$
$$+\Delta t\,\left(g\left(\nu_{j-1/2}^{n,+}, u_{j-1}^n, u_j^n\right) - \nu_{j-1/2}^n\,u_R\left(\nu_{j-1/2}^{n,+}, u_{j-1}^n, u_j^n\right)\right).$$

One can notice that when there is no phase transition, $\nu^n_{j-1/2} = \nu^n_{j+1/2} = 0$, $\Delta x = \Delta \overline{x}^n_j$ and we obtain the classical Godunov scheme. The last step is the sampling phase to define the solutions on the cells C^{n+1}_j. Following [7], for cell C^{n+1}_j we randomly pick a value between $\overline{u}^{n+1}_{j-1}$, $\overline{u}^{n+1}_j$ and $\overline{u}^{n+1}_{j+1}$ according to their rate of presence in cell C^{n+1}_j. This is done using the Van der Corput sequence $(a_n)_{n\in\mathbf{N}}$ (3.10) which is a low-discrepancy sequence in the interval $[0,1]$ (used in context of Glimm's scheme [8]).

$$u^{n+1}_j = \begin{cases} \overline{u}^{n+1}_{j-1} & \text{if } \ a_n \in]0, \max(\frac{\Delta t}{\Delta \overline{x}^n_j}\,\nu^n_{j-1/2}, 0)] \\ \overline{u}^{n+1}_j & \text{if } \ a_n \in] \max(\frac{\Delta t}{\Delta \overline{x}^n_j}\,\nu^n_{j-1/2}, 0), 1 + \min(\frac{\Delta t}{\Delta \overline{x}^n_j}\,\nu^n_{j+1/2}, 0)[\\ \overline{u}^{n+1}_{j+1} & \text{if } \ a_n \in [1 + \min(\frac{\Delta t}{\Delta \overline{x}^n_j}\,\nu^n_{j+1/2}, 0), 1[\end{cases} \tag{3.10}$$

REMARK 3.18. In the general case the congested domain Ω_c is not convex in (ρ, q) coordinates due to the convexity of the metastable border of the domain as illustrated on figure 3.4. It is therefore needed to add a projection step as a fourth step of the modified Godunov scheme, which does not affect its accuracy at the first order.

3.6. Error metric. The error metric chosen to assess the numerical accuracy of the scheme is the $L^1(\mathbf{R}, L^1(\mathbf{R}, \mathbf{R}^2))$ relative error between the computed solution and a wavefront tracking solution [4], which we assume to be the exact solution. We call u and u_c the exact and computed solutions respectively. For the computational domain $[x_0, x_1]$, the error at T is computed as follows:

$$E(T) = \frac{\int_0^T \int_{x_0}^{x_1} \|u(t,x) - u_c(t,x)\|_1 dx dt}{\int_0^T \int_{x_0}^{x_1} \|u(t,x)\|_1 dx dt}.$$

Following [5], we compute the value of a formal order of convergence γ as:

$$\gamma(M) = \log_2\left(\frac{e(1,M)}{e(2,M)}\right) \ \text{ with } \ e(p,M) = \frac{h}{p} \sum_{i=1\ldots pM} \|u_c^{\frac{h}{p}}(p\,N, i) - u_c^{\frac{h}{2\,p}}(2\,p\,N - 1, 2\,i - 1)\|_1$$

where u^h_c is the computed solution for a space step h, and the value of N is determined from the value of M by the *Courant-Friedrichs-Lewy* (CFL) condition [30].

4. The Newell-Daganzo model. In this section, we use a Newell-Daganzo velocity function for congestion, i.e. a velocity function for which the flux is affine with respect to the density. We instantiate the corresponding (ρ, q) model for this flux function and derive a corresponding Riemann solver, which we implement and test on benchmark cases.

4.1. Analysis of the equilibrium. According to the requirements detailed in § 3.1, we propose to use the following equilibrium function, which is the only function satisfying all these requirements, and yielding a flux affine with the density:

$$v^{eq}_c(\rho) = \frac{V\,\sigma}{R - \sigma}\left(\frac{R}{\rho} - 1\right).$$

This velocity function yields an affine flux, and the requirements on the vanishing point, trend, continuity and concavity property of the equilibrium flux are satisfied.

4.2. Analysis of the perturbation. In the general case, the velocity function reads:

$$\begin{cases} v_f(\rho) = V & \text{for } (\rho, q) \in \Omega_f \\ v_c(\rho, q) = \frac{V\,\sigma}{R-\sigma}\left(\frac{R}{\rho} - 1\right)(1+q) & \text{for } (\rho, q) \in \Omega_c \end{cases} \tag{4.1}$$

where Ω_f and Ω_c are defined by (3.5). The corresponding fundamental diagram is shown in figure 3.4. The equilibrium flux is affine with the density, but the 1-Lax curves outside the equilibrium are either convex or concave in $(\rho, \rho\, v)$ coordinates depending on the sign of the perturbation.

REMARK 4.1. Note that the expression of the velocity in figure 3.4 is given by (4.1), depends on the phase, and is therefore set-valued for $\rho > \sigma_-$ which is the lowest value of density for which congestion can arise. The conditions from § 3.2.2 to have positive speed and strict hyperbolicity of the congested part of the system (3.3) reduce to:

$$q_- > -1.$$

REMARK 4.2. As in the original Colombo phase transition model [10], the 1-Lax curves are LD for $q = 0$, and the direction of the rarefaction waves change according to the sign of q. This yields interesting physical interpretations, but makes the Riemann solver derived more complex than the the one derived for the model presented in the following section, as it can be seen by comparing § 4.3 and § 5.3.

REMARK 4.3. As illustrated on figure 3.4 the flux is linear in congestion at equilibrium as per the Newell-Daganzo flux function. In remark 3.2 we stated that this shape models neutral drivers (aggressivity-wise). When the traffic is above equilibrium, meaning that the velocity is higher that what it is for the same density at equilibrium, then the 1-Lax curves are concave in $(\rho, \rho\, v)$ coordinates, meaning that the drivers are more aggressive. So such a fundamental diagram shape seems to be in accordance with the intuition, that for a given density, if a set of speeds exists on the highway, the most aggressive drivers tend to be above the equilibrium velocity. This is symmetrically true for less aggressive drivers.

REMARK 4.4. It is also in accordance with the intuition that the lowest density for which congestion can arise is due to non-aggressive drivers (convex 1-Lax curves in $\rho = \sigma_-$). Indeed, the flux starts to decrease because some drivers are too careful and tend to drive not fast enough, which is not 'necessary' for an average driver.

4.3. Solution of the Riemann problem. Following [11],we construct the solution of the Riemann problem for the system (3.3) with the velocity function defined by (4.1) and the initial datum:

$$(\rho, q)(0, x) = \begin{cases} (\rho_l, q_l) & \text{if } x < 0 \\ (\rho_r, q_r) & \text{if } x > 0. \end{cases}$$

We note u the vector (ρ, q). We define u_m by the solution in Ω_c of the system:

$$\begin{cases} \frac{q_m}{\rho_m} = \frac{q_l}{\rho_l} \\ v_c(u_m) = v_c(u_r) \end{cases} \tag{4.2}$$

which yields a quadratic polynomial in ρ_m. We address the general case where the solution u_m of system (4.2) can coincide with u_l or u_r.

Case 1: $u_l \in \Omega_f$ and $u_r \in \Omega_f$
For all values of (ρ_l, ρ_r) the solution consists of a contact discontinuity from u_l to u_r.
Case 2: $u_l \in \Omega_c$ and $u_r \in \Omega_c$

(i) If $q_l > 0$ and $v_c(u_r) \geq v_c(u_l)$ the solution consists of a 1-rarefaction wave from u_l to u_m and a 2-contact discontinuity from u_m to u_r.

(ii) If $q_l > 0$ and $v_c(u_l) > v_c(u_r)$ the solution consists of a shock wave from u_l to u_m and a 2-contact discontinuity from u_m to u_r.

(iii) If $q_l = 0$ the solution consists of a 1-contact discontinuity from u_l to u_m and a 2-contact discontinuity from u_m to u_r.

(iv) If $0 > q_l$ and $v_c(u_r) > v_c(u_l)$ the solution consists of a shock wave from u_l to u_m and a 2-contact discontinuity from u_m to u_r.

(v) If $0 > q_l$ and $v_c(u_l) \geq v_c(u_r)$ the solution consists of a 1-rarefaction wave from u_l to u_m and a 2-contact discontinuity from u_m to u_r.

Case 3: $u_l \in \Omega_c$ and $u_r \in \Omega_f$

(i) If $0 > q_l$ the solution consists of a shock wave from u_l to u_m and of a contact-discontinuity from u_m to u_r.

(ii) If $q_l = 0$ the solution consists of a 1-contact discontinuity from u_l to u_m and of a contact-discontinuity from u_m to u_r.

(iii) If $q_l > 0$ the solution consists of a 1-rarefaction wave from u_l to u_m and of a contact-discontinuity from u_m to u_r.

Case 4: $u_l \in \Omega_f$ and $u_r \in \Omega_c$ Let u_{m-} be defined by the solution in Ω_c of the system:

$$\begin{cases} \frac{q_{m-}}{\rho_{m-}} = \frac{q_-}{R} \\ v_c(u_{m-}) = v_c(u_r) \end{cases}$$

and let $\Lambda(u_l, u_{m-})$ be the Rankine-Hugoniot phase transition speed between u_l and u_{m-} defined by equation (3.9).

(i) If $\Lambda(u_l, u_{m-}) \geq \lambda_1(u_{m-})$ the solution consists of a phase transition from u_l to u_{m-} and of a 2-contact discontinuity from u_{m-} to u_r.

(ii) If $\Lambda(u_l, u_{m-}) < \lambda_1(u_{m-})$ let u_p be defined by the solution in Ω_c of the system:

$$\begin{cases} \frac{q_p}{\rho_p} = \frac{q_-}{R} \\ \Lambda(u_l, u_p) = \lambda_1(u_p). \end{cases}$$

The solution consists of a phase transition from u_l to u_p, of a 1-rarefaction wave from u_p to u_{m-}, and of a 2-contact discontinuity from u_{m-} to u_r.

4.4. Benchmark test. In this section we compare the numerical results given by the modified Godunov scheme on a benchmark test in which the exact solution can be approximated almost exactly using wavefront tracking [4]. We use the phase transition model (3.3) in the Newell-Daganzo case (4.1) with the following choice of parameters: $V = 45$, $R = 1000$, $\sigma_- = 190$, $\sigma = 220$, $\sigma_+ = 270$. The benchmark test is a phase transition from free-flow to congestion (FF-C) with the following parameters:

(i) $u_l = (100, -0.6)$ which corresponds to free-flow with $\rho = 100$ and $v = 45$.

(ii) $u_r = (700, 0.5)$ which corresponds to a congested situation above equilibrium with $\rho = 700$ and $v = 8.2$.

This configuration gives rise to a phase transition between u_l and a congested state u_m followed by a 2-contact discontinuity between u_m and u_r (Riemann case 4, first

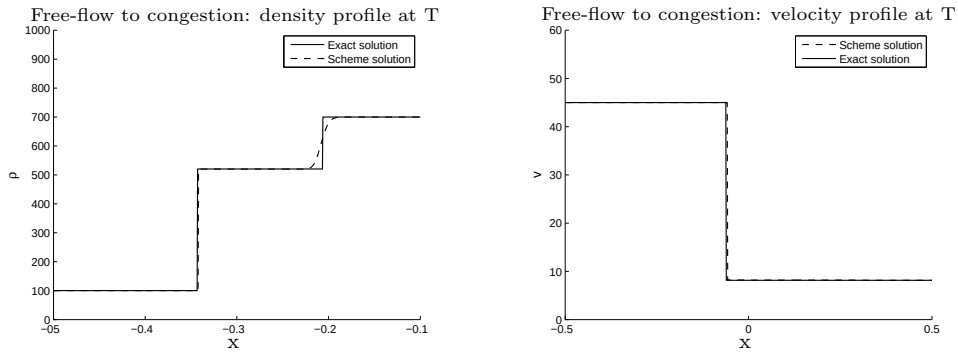

FIG. 4.1. *Exact solution (continuous line) and computed solution (dashed line) for density (left) and speed (right). Between the two initial state appears a state* $u_m = (474, -0.42)$ *which corresponds to the intersection of the lower bound of the diagram in congestion (1-Lax curve with* $q/\rho = q_-/R$*) with the 2-Lax curve* $v = v_c(u_l)$*. In this graph* $T = 0.55$ *and* $\Delta x = 0.0013$*.*

subcase), as shown in figure 4.1. The values of the error $E(T)$ and of the formal order of convergence γ, as described in § 3.6 for $T = 4$, (a typical time for which all interactions have moved out of the computational domain) are outlined in table 4.1.

Cell ♯	$E(T)$	$\gamma(T)$
50	$6.0\ 10^{-02}$	$4.4\ 10^{-01}$
100	$3.8\ 10^{-02}$	$5.6\ 10^{-01}$
200	$2.5\ 10^{-02}$	$5.7\ 10^{-01}$
400	$1.6\ 10^{-02}$	

TABLE 4.1

L^1 *relative error between exact solution and the modified Godunov scheme solution for the test cases explicitly described above, and formal order of convergence, for different discretization.*

5. The Greenshields model. In this section we use a Greenshields model to describe the velocity function in congestion, i.e. we use a concave quadratic flux function. First we study the equilibrium flux function, then we present the associated perturbed model, and finally we derive the corresponding Riemann solver which we test on a benchmark case.

5.1. Analysis of the equilibrium. We use a quadratic relation to describe the congestion equilibrium, which because of physical considerations needs to satisfy the requirements from § 3.1. This leads us to choose the flux as a quadratic function of the form:

$$\rho\, v_c^{eq}(\rho) = (\rho - R)\,(a\,\rho + b)$$

such that the vanishing condition at $\rho = R$ is satisfied. Continuity at the critical density σ yields:

$$b = \frac{\sigma\, V}{\sigma - R} - a\,\sigma$$

so the flux at equilibrium reads:

$$\rho\, v_c^{eq}(\rho) = (\rho - R)\,\left(a\,(\rho - \sigma) + \frac{\sigma\, V}{\sigma - R}\right)$$

with a variation interval for a defined by the second and third conditions of § 3.1 as:

$$a \in \left[-\frac{\sigma V}{(\sigma - R)^2}, 0 \right[.$$

Note that for the specific case in which $R = 2\,\sigma$ and a is defined by the fact that the derivative of the flux equals zero at σ (which reads $a = -\sigma V/(\sigma - R)^2$), we obtain the classical Greenshields flux.

5.2. Analysis of the perturbation. In this section, we analyze a flux function which is a Newell-Daganzo function in free-flow and a Grenshields function at the equilibrium in congestion. In agreement with the expression of the equilibrium obtained in § 5.1, and following the general form given in system (3.4), we write the perturbed velocity as:

$$\begin{cases} v_f(\rho) = V & \text{for } (\rho, q) \in \Omega_f \\ v_c(\rho, q) = \left(1 - \frac{R}{\rho}\right) \left(a\,(\rho - \sigma) + \frac{\sigma V}{\sigma - R}\right) (1 + q) & \text{for } (\rho, q) \in \Omega_c \end{cases} \tag{5.1}$$

with $a \in \left[-\frac{\sigma V}{(\sigma - R)^2}, 0 \right[$, and where Ω_f and Ω_c are defined by (3.5). The corresponding fundamental diagram is presented in figure 5.1.

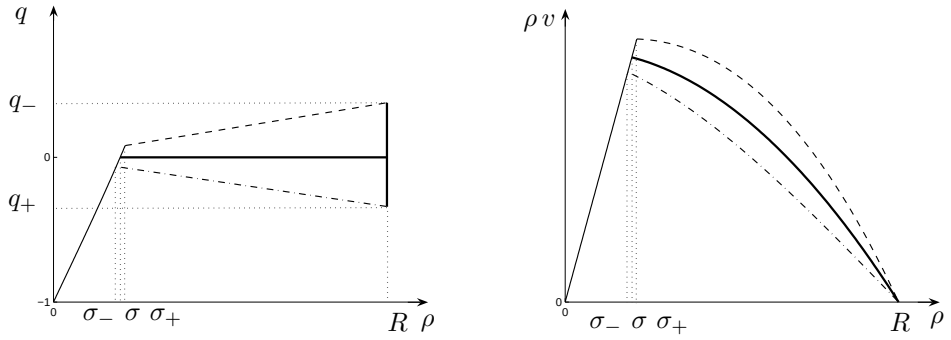

FIG. 5.1. ***Phase transition model with a Greenshields equilibrium. Left:*** *State-space coordinates.* ***Right:*** *Flux-density coordinates. Thin solid line: Free-flow. Bold solid line: Congestion equilibrium. Thin dashed line: Upper bound of congestion. Thin dot-dashed line: Lower bound of congestion. The equilibrium flux is concave, and all the 1-Lax curves are concave in* $(\rho, \rho\,v)$ *coordinates.*

REMARK 5.1. The expression of the velocity function given by system (5.1) enables a set-valued velocity function for $\rho > \sigma_-$. For a given density the variable velocity can take several values. The lower bound of congestion is concave, unlike for the model presented in § 4. This feature may be more appropriate for usual experimental datasets.

REMARK 5.2. Since all the 1-Lax curves are concave in $(\rho, \rho\,v)$ coordinates, unlike for the original phase transition model, the rarefactions always go left in $(\rho, \rho\,v)$ coordinates as it is the case for concave fluxes usually used in traffic [23, 34]. Another consequence of the constant concavity of the 1-Lax curves is that the Riemann solver is much simpler than in the Newell-Daganzo case, as detailed in § 5.3.

REMARK 5.3. According to remark 3.2 this flux function models aggressive drivers only. It is able to model a class of cloud of points observed experimentally where the congested domain has a concave lower border in $(\rho, \rho,\, v)$ coordinates.

The requirements from § 3.2.2 here reduce to:

$$q_- > -\frac{a\,R}{\frac{\sigma\,V}{\sigma - R} + a\,(2\,R - \sigma)}.$$

REMARK 5.4. It is interesting to note that while before the bound on the perturbation was given by the fact that the speed had to be positive, here the bound is tighter because we want also to have all the 1-Lax curves with constant concavity.

REMARK 5.5. The lower bound on the perturbation is an increasing function of the parameter a, so this parameter should be chosen as small as possible to allow for more liberty, namely $a_{\min} = -\sigma\,V/(\sigma - R)^2$ which yields the lowest bound on $q_-^{\min} = R/(2\,\sigma - 3\,R)$.

5.3. Solution of the Riemann problem. We consider the Riemann problem for system (3.3) with the velocity function from equation (5.1) and the initial datum:

$$(\rho, q)(0, x) = \begin{cases} (\rho_l, q_l) & \text{if } x < 0 \\ (\rho_r, q_r) & \text{if } x > 0. \end{cases} \tag{5.2}$$

We follow the method used in [11] to construct the solution. We define u_m by the solution in Ω_c of the system:

$$\begin{cases} \frac{q_m}{\rho_m} = \frac{q_l}{\rho_l} \\ v_c(u_m) = v_c(u_r) \end{cases} \tag{5.3}$$

which yields a quadratic polynomial in ρ_m with one root in $[0, R]$. In the general case, the solution u_m of the system (5.3) can be equal to u_l or u_r.

Case 1: $u_l \in \Omega_f$ and $u_r \in \Omega_f$ For all values of (ρ_l, ρ_r) the solution consists of a contact discontinuity from u_l to u_r.

Case 2: $u_l \in \Omega_c$ and $u_r \in \Omega_c$

(i) If $v_c(u_r) \geq v_c(u_l)$ the solution consists of a 1-rarefaction wave from u_l to u_m and a 2-contact discontinuity from u_m to u_r.

(ii) If $v_c(u_l) > v_c(u_r)$ the solution consists of a shock wave from u_l to u_m and a 2-contact discontinuity from u_m to u_r.

Case 3: $u_l \in \Omega_c$ and $u_r \in \Omega_f$ The solution consists of a 1-rarefaction wave from u_l to u_m and of a contact-discontinuity from u_m to u_r.

Case 4: $u_l \in \Omega_f$ and $u_r \in \Omega_c$ Let u_{m-} be defined by the solution in Ω_c of the system:

$$\begin{cases} \frac{q_{m-}}{\rho_{m-}} = \frac{q_-}{R} \\ v_c(u_{m-}) = v_c(u_r) \end{cases}$$

and let $\Lambda(u_l, u_{m-})$ be the Rankine-Hugoniot phase transition speed between u_l and u_{m-} defined by equation (3.9). The solution consists of a phase transition from u_l to u_{m-} and of a 2-contact discontinuity from u_{m-} to u_r.

REMARK 5.6. One can note that in this case, the Riemann problem is particularly simple, with only five different types of solutions, compared to the Newell-Daganzo case which has eleven different types of solutions.

REMARK 5.7. The analysis in the case of a convex equilibrium flux function, which we do not address in this article is closely related to this case, modulo the sign of the parameter a and the concavity of the 1-Lax curves.

5.4. Benchmark test. In this section we compare the numerical results given by the modified Godunov scheme on a benchmark test considering a wavefront tracking solution [4] to be the exact solution. We use the phase transition model (3.3) in the Greenshields case (5.1) with the following choice of parameters: $V = 45$, $R = 1000$, $\sigma_- = 188$, $\sigma = 200$, $\sigma_+ = 215$. We also choose $a = -0.01$. The resulting values for the extrema of the perturbation are $q_- = -0.34$ and $q_+ = 0.38$. The benchmark test is a phase transition from free-flow to congestion, with the following parameters:

(i) $u_l = (150, -0.26)$ which corresponds to $\rho = 150$ and $v = 45$.

(ii) $u_r = (300, -0.02)$ which corresponds to a congested situation under equilibrium with $\rho = 300$ and $v = 28$.

This configuration gives rise to a phase transition between u_l and a congested state u_m followed by a 2-contact discontinuity between u_m and u_r (Riemann case 4) which is illustrated in figure 5.2. Table 5.1 summarizes the values of the error $E(T)$, and the

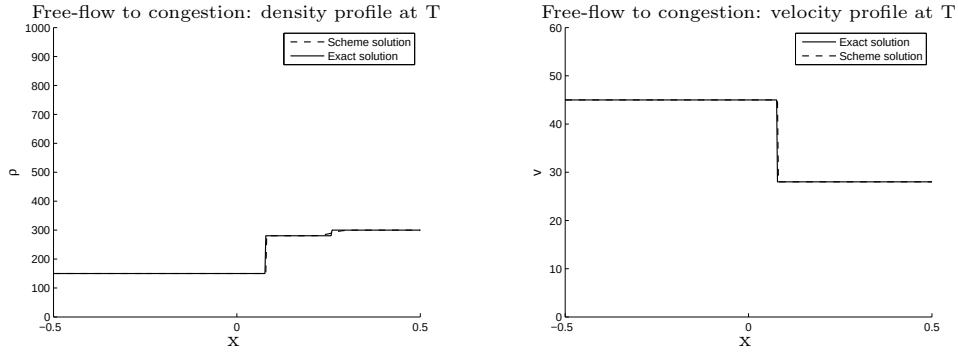

FIG. 5.2. *Exact solution (continuous line) and computed solution (dashed line) for density (left) and speed (right). Between the two initial state appears a state* $u_m = (280.6, -0.094)$ *which corresponds to the intersection of the lower bound of the diagram in congestion. In this graph* $T = 0.37$ *and* $\Delta x = 0.0025$.

formal order of convergence γ, as defined in § 3.6, for different size of the discretization step, at $T = 4$.

Cell ♯	$E(T)$	$\gamma(T)$
50	$3.5\ 10^{-03}$	3.7
100	$1.9\ 10^{-03}$	-1.8
200	$1.0\ 10^{-03}$	3.0
400	$5.7\ 10^{-04}$	

TABLE 5.1

L^1 relative error between exact solution and the modified Godunov scheme solution for the test cases explicitly described above, and for different number of space cells.

6. Conclusion. This article reminded the fundamental features of the Colombo phase transition model, which were extended to construct a class of models in which the fundamental diagram is set-valued in the congested regime. The notion of equilibrium which provides the basis for the construction of the 2×2 phase transition models was introduced. General conditions which enable the extension of the original Colombo phase transition model to this new class of 2×2 phase transition models were investigated. A modified Godunov scheme which can be applied to models with non-convex state-space was used to solve these equations numerically. The model was

instantiated for two specific flux functions, which include the Newell-Daganzo flux function (affine) and the Greenshields flux function (quadratic concave). A discussion of the choice of parameters needed for each of the models was conducted. The solution of the Riemann problem was derived, and a validation of the numerical results using benchmark tests was conducted. Wavefront tracking methods were assumed to provide an almost exact solution, which was used for comparison with the numerical solution. Open questions for this model include the capability of the model to accurately reproduce traffic features experimentally measured on highways, which is the focus of ongoing work. Experimental validations of the model should reveal its capabilities of reproducing traffic flow more accurately than existing models. In addition, the specific potential of the model to integrate velocity measurements (through proper treatment of the second state variable of the problem) is a significant advantage of this model over any first order model for which the density-flux relation is single valued. The proper use of this key feature for data assimilation is also an open problem, which could have very promising outcomes for highway traffic state estimation.

REFERENCES

[1] A. Aw and M. Rascle, *Resurrection of "second order" models of traffic flow*, SIAM J. Appl. Math., 60 (2000), pp. 916–938.

[2] C. Bardos, A.-Y. Leroux, and J.-C. Nedelec, *First order quasilinear equations with boundary conditions*, Comm. Partial Differential Equations, 4 (1979), pp. 1017–1034.

[3] S. Blandin, G. Bretti, A. Cutolo, and B. Piccoli, *Numerical simulations of traffic data via fluid dynamic approach*, Appl. Math. Comput., (2009 (to appear)).

[4] A. Bressan, *Hyperbolic systems of conservation laws: the one-dimensional Cauchy problem*, Oxford University Press, Oxford, UK, 2000.

[5] G. Bretti, R. Natalini, and B. Piccoli, *Fast algorithms for the approximation of a traffic flow model on networks*, Discrete Contin. Dyn. Syst. Ser. B, 6 (2006), pp. 427–448.

[6] M. Cassidy and J. Windover, *Methodology for assessing dynamics of freeway traffic flow*, Transportation Research Record, 1484 (1995), pp. 73–79.

[7] C. Chalons and P. Goatin, *Godunov scheme and sampling technique for computing phase transitions in traffic flow modeling*, Interfaces and Free Boundaries, 10 (2008), pp. 195–219.

[8] P. Collela, *Glimm method for gas dynamics*, SIAM Journal on Scientific and Statistical Computing, 3 (1982), pp. 76–110.

[9] R. Colombo, *On a 2 × 2 hyperbolic traffic flow model*, Math. Comput. Modelling, 35 (2002), pp. 683–688.

[10] ———, *Hyperbolic phase transitions in traffic flow*, SIAM J. Appl. Math., 63 (2003), pp. 708–721.

[11] R. Colombo, P. Goatin, and F. Priuli, *Global well-posedness of traffic flow models with phase transitions*, Nonlinear Analysis, 66 (2007), pp. 2413–2426.

[12] C. Daganzo, *The cell transmission model: a dynamic representation of highway traffic consistent with the hydrodynamic theory*, Transportation Research Part B, 28 (1994), pp. 269–287.

[13] ———, *The cell transmission model, part ii: Network traffic*, Transportation Research Part B, 29 (1995), pp. 79–93.

[14] ———, *Requiem for second-order fluid approximations of traffic flow*, Transportation Research Part B, 29 (1995), pp. 277–286.

[15] C. Daganzo, M. Cassidy, and R. Bertini, *Possible explanations of phase transitions in highway traffic*, Transportation Research Part A, 33 (1999), pp. 365–379.

[16] J. Del Castillo and F. Benitez, *On the functional form of the speed-density relationship i: General theory*, Transportation Research Part B, 29 (1995), pp. 373–389.

[17] J. Del Castillo, P. Pintado, and F. Benitez, *The reaction time of drivers and the stability of traffic flow*, Transportation research. Part B, 28 (1994), pp. 35–60.

[18] M. Garavello and B. Piccoli, *Traffic flow on networks*, American Institute of Mathematical Sciences, Springfield, USA, 2006.

[19] ———, *On fluido-dynamic models for urban traffic*. Submitted to Transportation Research B, 2008.

[20] J. Glimm, *Solutions in the large for nonlinear hyperbolic systems of equations*, Comm. Pure Appl. Math., 18 (1965), pp. 697–715.
[21] S. Godunov, *A difference method for numerical calculation of discontinuous solutions of the equations of hydrodynamics*, Sb. Math., 89 (1959), pp. 271–306.
[22] H. Greenberg, *An analysis of traffic flow*, Oper. Res., 7 (1959), pp. 79–85.
[23] B. Greenshields, *A study of traffic capacity*, Proceedings of the Highway Research Board, 14 (1935), pp. 448–477.
[24] Z. Jia, C. Chen, B. Coifman, and P. Varaiya, *The pems algorithms for accurate, real-time estimates of g-factors and speeds from single-loop detectors*, in Intelligent Transportation Systems, 2001. Proceedings. 2001 IEEE, 2001, pp. 536–541.
[25] B. Kerner, *Experimental features of self-organization in traffic flow*, Phys. Rev. Lett., 81 (1998), pp. 3797–3800.
[26] ———, *Phase transitions in traffic flow*, Traffic and granular flow, (2000), pp. 253–283.
[27] S. Kruzhkov, *First order quasilinear equations in several space variables*, Sb. Math., 10 (1970), pp. 217–243.
[28] L. Tong, *Nonlinear dynamics of traffic jams*, Phys. D, 207 (2005), pp. 41–51.
[29] P. Le Floch, *Explicit formula for scalar non-linear conservation laws with boundary conditions*, Mathematical methods in the applied sciences, 10 (1988), pp. 265–287.
[30] R. Leveque, *Finite volume methods for hyperbolic problems*, Cambridge University Press, Cambridge, UK, 1992.
[31] M. Lighthill and G. Whitham, *On kinematic waves ii a theory of traffic flow on long crowded roads*, Proc. R. Soc. Lond. Ser. A Math. Phys. Eng. Sci., 229 (1956), pp. 317–345.
[32] W. Lin and D. Ahanotu, *Validating the Basic Cell Transmission Model on a Single Freeway Link*, Institute of Transportation Studies, University of California, Berkeley, California PATH technical report 95-3, 1995.
[33] L. Munoz, X. Sun, R. Horowitz, and L. Alvarez, *Traffic density estimation with the cell transmission model*, in American Control Conference, 2003. Proceedings of the 2003, vol. 5, 2003.
[34] G. Newell, *A simplified theory of kinematic waves in highway traffic ii: Queueing at freeway bottlenecks*, Transportation research Part B, 27 (1993), pp. 289–303.
[35] O. Oleinik, *Discontinuous solutions of non-linear differential equations*, Uspekhi Mat. Nauk, 12 (1957), pp. 3–73.
[36] M. Papageorgiou, *Some remarks on macroscopic traffic flow modelling*, Transportation Research Part A, 32 (1998), pp. 323–329.
[37] H. Payne, *Models of freeway traffic and control*, Simulation Councils, Inc., 1971.
[38] P. Richards, *Shock waves on the highway*, Oper. Res., 4 (1956), pp. 42–51.
[39] D. Serre, *Systems of conservation laws*, Diderot, Paris, France, 1996.
[40] I. Strub and A. Bayen, *Weak formulation of boundary conditions for scalar conservation laws: an application to highway traffic modelling*, Internat. J. Robust Nonlinear Control, 16 (2006), pp. 733–748.
[41] B. Temple, *Systems of conversation laws with invariant submanifolds*, Trans. Amer. Math. Soc., 280 (1983), pp. 781–795.
[42] E. Toro, *Riemann solvers and numerical methods for fluid dynamics*, Springer-Verlag, New-York, USA, 1997.
[43] R. Underwood, *Speed, volume, and density relationships: Quality and theory of traffic flow*, Yale Bureau of Highway Traffic, (1961), pp. 141–188.
[44] P. Varaiya, *Reducing highway congestion: an empirical approach*, Eur. J. Control, 11 (2005), pp. 301–309.
[45] ———, *Congestion, ramp metering and tolls*, Philos. Trans. R. Soc. Lond. Ser. A Math. Phys. Eng. Sci., 366 (2008), pp. 1921–1930.
[46] Y. Wang and M. Papageorgiou, *Real-time freeway traffic state estimation based on extended kalman filter: a general approach*, Transportation Research Part B, 39 (2005), pp. 141–167.
[47] G. Whitham, *Linear and Nonlinear Waves*, Pure Appl. Math. (N. Y.), 1974.
[48] H. Zhang, *A theory of nonequilibrium traffic flow*, Transportation Research Part B, 32 (1998), pp. 485–498.
[49] ———, *A non-equilibrium traffic model devoid of gas-like behavior*, Transportation Research Part B, 36 (2002), pp. 275–290.